ACCSCIENCE PUBLISHING

Materials Science in Additive Manufacturing

ORIGINAL RESEARCH ARTICLE

Fast layer fiber orientation optimization method for continuous fiber-reinforced material extrusion process

Valentin Marchal, Yicha Zhang*, Nadia Labed, Rémy Lachat, and François Peyraut

Laboratoire Interdisciplinaire Carnot de Bourgogne, Unité Mixte de Recherche 6303, Centre National de la Recherche Scientifique, Université de Bourgogne Franche-Comté, Université de Technologie de Belfort-Montbéliard, F-90010 Belfort, France

Abstract

Material extrusion (MEX) is an additive manufacturing process that uses thermoplastic layer-by-layer building. The use of continuous fiber-reinforced filament enhances mechanical properties, making MEX suitable for use in aerospace, automotive, and robotics industries. This study proposes a laminate optimization method to improve the stiffness of printed parts with low computing time. The 2D stress-flow-based method optimizes fiber's orientation for each layer in the stacking direction, giving results for a 3D part optimization in a few minutes. Developed with Ansys Parametric Design Language, the computation tool was tested on printed wrenches, resulting in an 18% increase in stiffness. The proposed method is applicable to any printable shape.

Keywords: Additive manufacturing; Continuous fiber printing; Finite element method; Optimization

***Corresponding author:**
Yicha Zhang
(yicha.zhang@utbm.fr)

Citation: Marchal V, Zhang Y, Labed N, *et al.*, 2023, Fast layer fiber orientation optimization method for continuous fiber-reinforced material extrusion process. *Mater Sci Add Manuf,* 2(1): 49.
https://doi.org/10.36922/msam.49

Received: February 1, 2023

Accepted: February 15, 2023

Published Online: March 17, 2023

1. Introduction

Composite materials have seen significant growth since their creation in the 1930s, with applications ranging from experimental parts to mass production. Polymer-based composites, known for their lightweight, corrosion resistance, and high stiffness, are widely used in aerospace, military, wind turbines, and automotive industries[1]. There are two types of fiber-reinforced polymers, short fiber reinforcement or long fiber reinforcement, compatible with various fiber such as carbon, glass, and aramid. Long-fiber reinforcement is the most promising for creating light parts with metal alloy-like properties[2]. However, traditional manufacturing processes are difficult and require expensive equipment. In contrast, additive manufacturing has experienced significant growth in recent decades, with several processes available including material extrusion (MEX), powder bed fusion (PBF), sheet lamination (SHL), binder jetting, directed energy deposition, material jetting, and vat photopolymerization (VPP)[3]. Four of these processes have been adapted to fiber-reinforced polymers (PBF[4-6], VPP[7], SHL, and MEX[7-9]), but MEX is the only one widely developed with continuous fiber reinforcement[3,9-11]. The MEX process builds parts layer by layer by fusing a thermoplastic filament fed into a printing nozzle by an extruder. The nozzle, controlled by three stepper motors for precise movement in the printing volume, follows routes defined by a slicer software using a

computer-aided design model of the part in.stl or.obj format. Optimal printing can be achieved by adjusting parameters, such as layer height, printing temperature, and bed temperature (if equipped). The optimal values of these printed parameters depend on the printed material, nozzle diameter, and ambient air temperature. MEX is attractive due to its ease of use, compatibility with various thermoplastics, low cost (for both printer and materials), and low energy consumption. When combined with continuous fiber-reinforced filaments, the MEX process leverages the benefits of both additive manufacturing and long fiber composites, resulting in complex freeform parts with stiffness comparable to aluminum alloys, low density, and corrosion resistance[12].

However, additive manufacturing of long fiber composites results in highly anisotropic materials. Hence, aligning the fibers with the mechanical strain is crucial to obtain the best stiffness and strength in a printed part[13-15]. Therefore, non-optimized fiber paths can lead to easy breakage. While previous works have explored fiber optimization, they have limitations. Zhou *et al.*[16] proposed a 2D model that divided the part into areas, each with a specific fiber orientation. Ding *et al.*[17] designed curved fiber routes using a 2D model. Li *et al.*[18] combined the two approaches with areas divided into concentric curved fiber routes. Safonov[19] and Nomura *et al.*[20] developed curved fiber routing in both 2D and 3D models, and Jung *et al.*[21] created a complex model that considers fiber orientation and diameter. All these methods are stress-based and consider fiber to be most effective when its direction aligns with the major principal direction. However, they are not easily applied to commercial printers like Markforged or Anisoprint, and while they can be done with the open-source slicing software Aura, they require manual coding of fiber routes in a gcode file. In addition, slicers like Eiger or Aura work layer-by-layer, a constraint of the MEX process that makes it impossible to use 3D optimization models and makes it challenging to find an easy and quick optimization model for commercial printers. To solve the problem above, the best fiber orientation is determined using a standard stress flow method based on principal stress analysis and corresponding direction. Keeping ease of use for commercial printers in mind, the concept of a stack is introduced: A set of layers with optimized orientation angles for each layer, weighted by the dominant principal stress. A cost-optimization approach using a multi-layered finite element model and the previously computed best orientation angles is also proposed. This allowed the identification of a reduced number of layers, where reinforcement is necessary, while using nylon in other layers. The methodology, implemented in Ansys Parametric Design Language, was efficient and demonstrated by a 18% increase in stiffness of wrenches manufactured on a Markforged X7 printer, without the need for time-consuming topology optimization algorithms or metamodels.

2. Principal stress-based method

Since printed composite parts are built layer-by-layer, resulting in a laminate composite, fibers are not oriented in a 3D space but in a stacking way. Intuitively, a 2D method applied to each layer of a part seems to be well adapted. However, this could result in a huge simulation cost, as MEX layers are thin (close to a tenth millimeter). For example, optimization of a ten-centimeter-high part would result in a thousand optimization processes. Furthermore, commercial machines only allow one angle per layer for oriented fibers. To solve these two issues, we will not consider a 2D layer-based method, but a 3D method based on a stack division of the part, as explained later.

2.1. 3D model based on a stack division of the part

To meet the time computation needs of designers, we introduce the concept of a stack, which is a group of several layers. By working with stacks instead of individual layers, we can decrease the mesh size and significantly reduce computation time. For example, a ratio of ten between a layer-based mesh and a stack-based mesh results in a 3D mesh that is 1000 times lighter (Figure 1). Working with stacks of ten layers provides a good balance between efficient computation and accurate results from the finite element analysis, as values greater than ten result in significant loss of precision. Hence, based on this simplification concept, an optimization method is proposed to optimize the fiber angles for each stack of layers as an optimal configuration to improve the structure's stiffness and strength.

Besides an important reduction of the simulation cost, using a stack-based 3D model also allows the user to allocate different angles on the layers of a stack while a layer-based model allows only one angle per layer. Thus, if a layer-based model is considered, each layer is reinforced with only the dominant stress orientation (Figure 2B left). However, some mechanical loads may result in a complex stress flow, with several strained directions (Figure 2A). As additively manufactured composites have low stiffness and strength when the load is not aligned with the fibers, it is important to consider all the possible strained orientations, as our model allows (Figure 2B right). With our approach, the computed percentages represented by each orientation (20%, 30%, and 50%) are distributed in ten different layers, so each area is reinforced on at least one layer.

2.2. Optimization process

This section presents our optimization process with the different substeps included in the workflow (Figure 3). It is

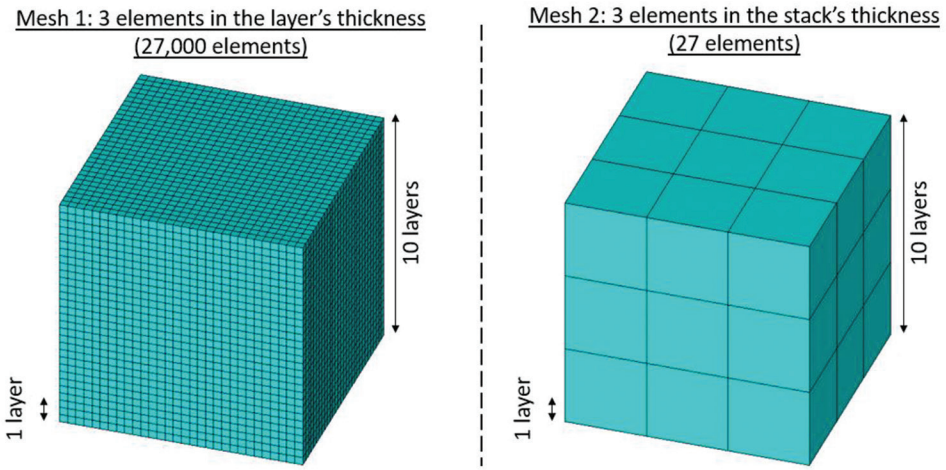

Figure 1. Comparison of number of layer-dimensioned mesh (left) and a stack-dimensioned mesh (right) on the same volume.

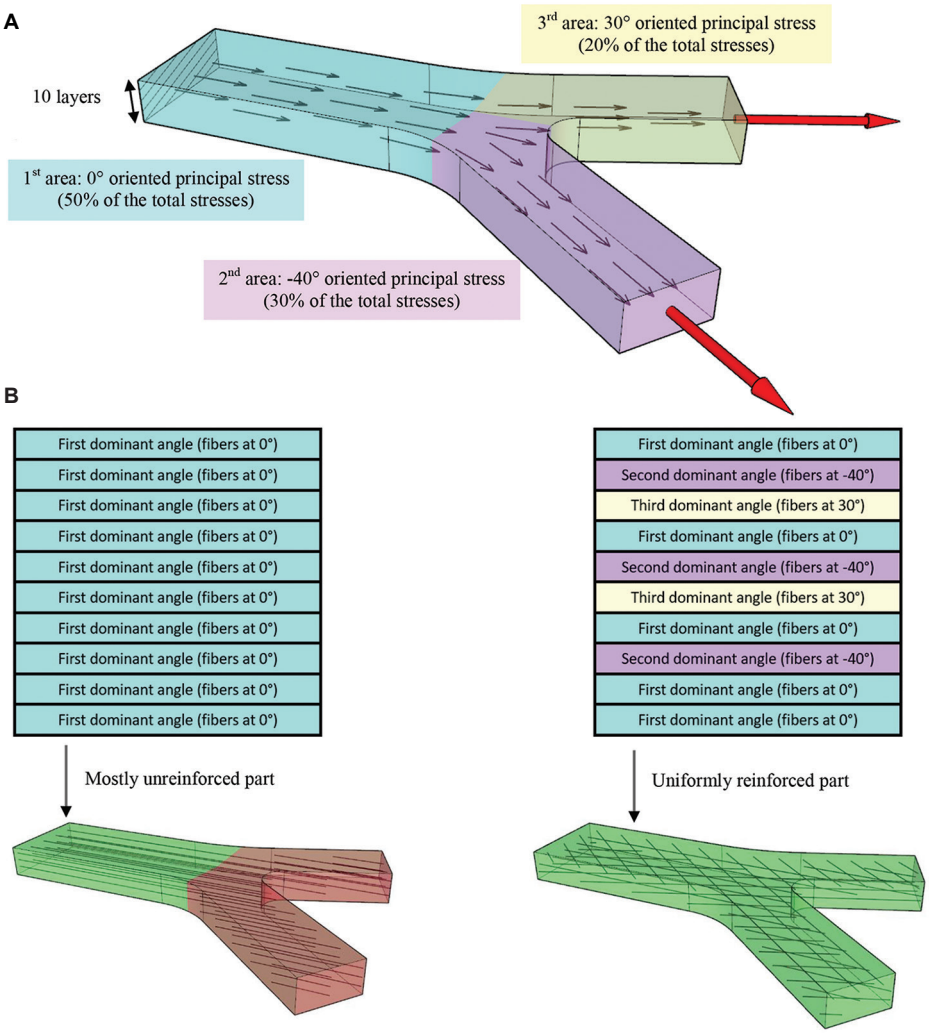

Figure 2. (A) Identification of the principal directions for a structure. (B) Fiber angle assignment for a layer-based optimized orientation (left) and a stack-based optimized orientation (right).

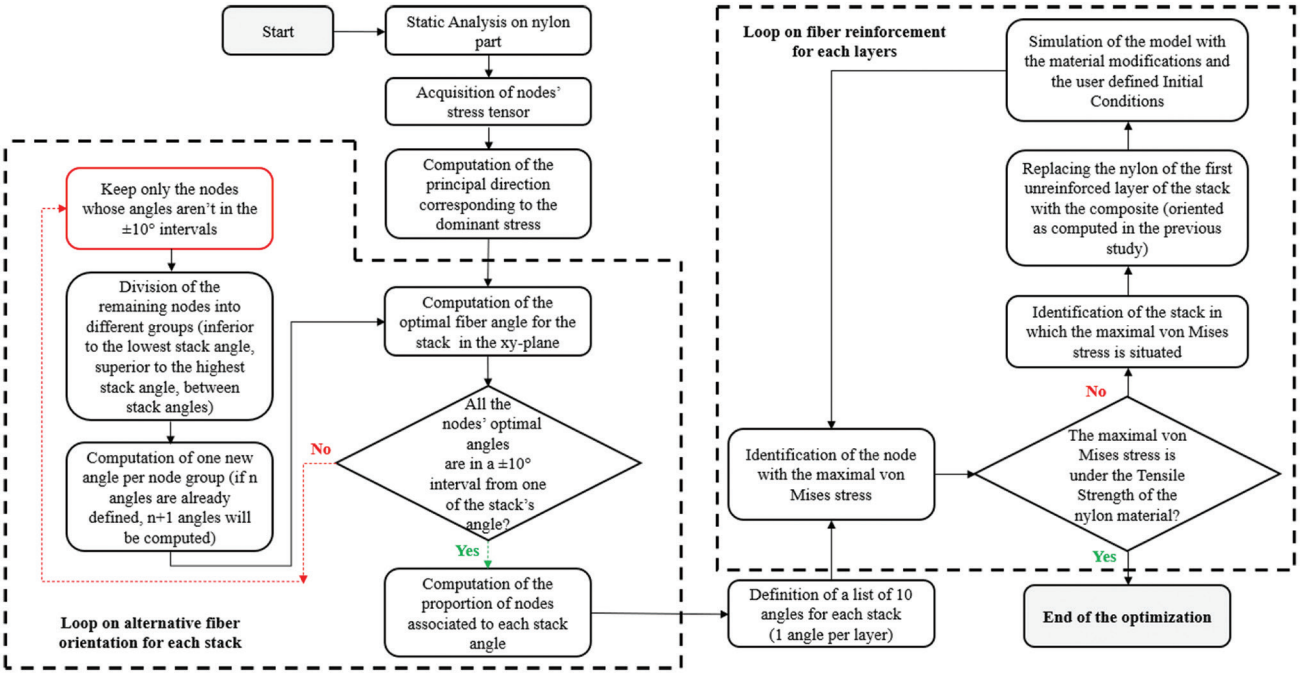

Figure 3. Flow chart of computation of the optimal stack's fiber angles and of the number of reinforced layers.

divided into two steps: The first one is to define an optimal fiber angle sequence for each stack of ten layers, and the second one is to optimize the number of reinforced layers.

2.2.1. Optimized stack fiber angles

The first step of our proposed method is to determine the optimal fiber angle based on the intuitive idea, considering that the optimal fiber orientation of the material should coincide with the absolute value of the dominant principal stress direction[16]. This method includes several substeps as shown in the workflow (Figure 3):

(i) A static analysis is first run on a whole part made of an isotropic material. This first calculation allows to determine the location where the deposit of fibers is needed to reinforce the stiffness of the part. After this static analysis is performed, the Cauchy stress tensor of each node is obtained.

(ii) The diagonalization of the Cauchy stress tensor gives the three principal stresses and the three principal directions. As the fibers in a composite are efficient for tensile or compressive loads, the first principal stress (tensile stress) is compared to the absolute value of the third principal stress (compressive if negative) to determine which of these two situations should be considered.

(iii) The principal direction corresponding to the dominant stress in absolute value between the first and third principal stress is used to compute the fiber orientation. The principal direction is projected on the xy-plane (perpendicular to the stacking direction z) because the current commercial manufacturing process does not allow printing continuous fibers in 3D orientations but only in 2D layers. The angle between this projected direction and the X-axis (considered parallel to a 0° fiber's orientation) is computed at each node of the mesh. The optimal fiber angle of the stack is the mean value of the node's fiber angles, weighted by the dominant principal stress value of each node.

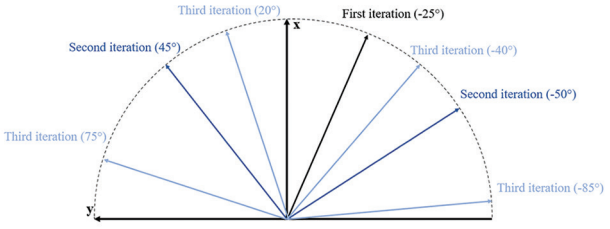

Figure 4. Computation of the stack's fiber angles iteration by iteration.

(iv) To account for a possible deviation around the mean value calculated in step (iii), the algorithm determines which node has a fiber angle more than 10° degrees greater or lower than this mean value. Note that the value of 10° can be decreased at will by the user, but it should not be increased, as it has been found that the strength and the stiffness fall quickly when the angle between the fibers and the load exceed 10°. The remaining nodes are divided into two areas (upper and lower to the mean value), giving two new mean angles (Figure 4). While node's fiber angles are not in

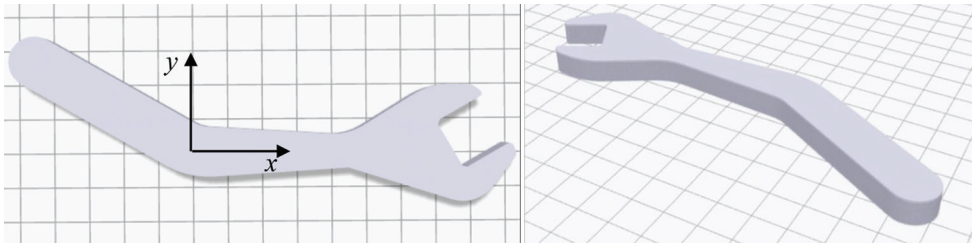

Figure 5. Top (left) and isometric (right) views of the wrench.

the interval of 10° width around the mean value, a new iteration is made.

Hence, a sequence of 10 fiber angles for each stack is obtained at the end of this first step. This result is used as an input for the second step.

2.2.2. Optimized number of reinforced layers

Once the optimal fiber's orientation has been computed inside each stack, it is necessary to reduce as much as possible the number of reinforced layers because continuous fiber-reinforced filament is a more expensive and heavier material compared to the nylon, which is also available with the Markforged X7 printer used in this work. To perform this cost reduction, a multi-layered finite element model only containing nylon at the beginning is used. A first computation provides the stacks where the maximal von Mises stress is located inside the nylon layers. While this maximal von Mises stress is higher than the tensile strength of the nylon, the material of the first unreinforced layer of the stack is replaced by the composite, oriented with the angle computed for this layer in the previous study. If there are locations where the von Mises stress is higher than the tensile strength of the nylon, the loop starts again.

3. Case study

The specific case of a wrench, which is an easy-to-print part (Figure 5), is considered. The crooked handle, with an angle of 30° between the two sections, makes the stress flow more complex and more interesting to study than a straight handle with unidirectional fiber reinforcement. Intuitively, the best way to enhance the stiffness of the wrench would be to reinforce equally the two sections, which would result in a 0°/−30° laminate. However, we will see in the next section that two additional angles calculated by our algorithm play a key role in the stiffness improvement.

3.1. Numerical results

The wrench is locked on the faces, which are supposed to be in contact with the screw, and a force is applied on the top of the handle (Figure 6). These boundary conditions

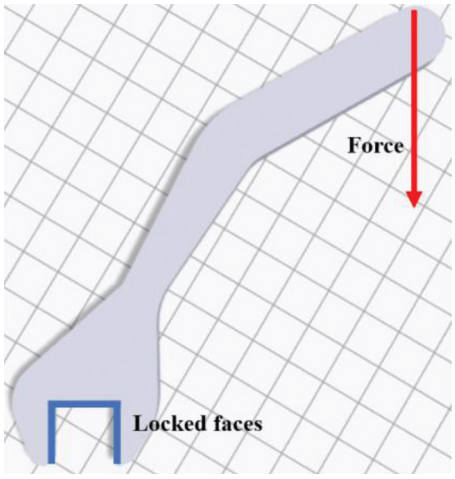

Figure 6. Mechanical model of the wrench.

correspond to the mechanical tests that we performed on the printed part.

The optimization model presented in section 2.2 gave the same fibers angle repartition for each stack with the following distribution: 2° (70%), −33° (10%), −17° (10%), and 13° (10%). The two angles of 0° and −30° that could be guessed intuitively were therefore found by the first step of the optimization algorithm depicted in Figure 3 with an angle of 2° close to 0° and an angle of −33° close to −30°. Since the stress' magnitudes were higher in the horizontal section of the handle (frame no. 2 in Figure 7) compared to the ones in the inclined section of the handle (frame no. 1 in Figure 7), the angle of 2° was logically more represented (seven times) than the angle of −33° corresponding to the inclined section. It is also important to note that the model gave two other angles (13° and −17°) corresponding to the stress fields inside of the wrench's head (frames no. 3 and no. 4, respectively, in Figure 7). The tests performed on the printed part demonstrated that these two additional angles that cannot be predicted without the help of an optimization algorithm play a key role to stiffen the wrench.

3.2. Tests on printed parts

To check whether the proposed method leads to an improvement of the performances of the wrench, two

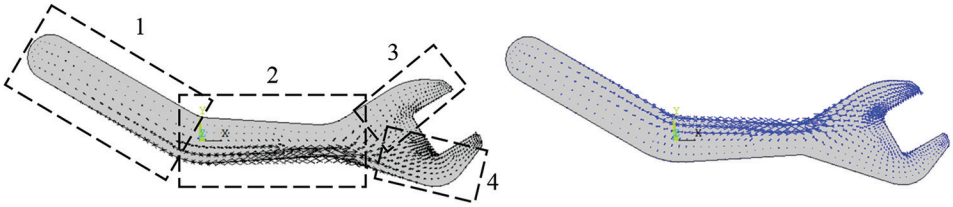

Figure 7. Distribution of the principal directions. Left: Tensile stress. Right: Compressive stress.

sets of printed parts were tested and then compared. The first set was built with an alternation of −30° oriented fibers (Figure 8A) and 0° oriented fibers (Figure 8B), corresponding to the intuitive fiber orientation. The second set has an alternation of the optimized angles computed in section 3.1 with the corresponding percentage: Seven layers with 2° oriented fiber, one layer at −33°, one layer at −17° and one layer at 13°. The parts were printed with a Markforged X7 printer using a continuous carbon fiber filament (blue routes on Figure 8). A nylon filament (white routes on Figure 8) was used for the roof and floor layers, which are mandatory with this printer.

Each wrench contains the same fiber content, only the orientation of the fiber changes. To be able to estimate the dispersion on the test results, three wrenches were printed for each fiber laminate. The six parts were tested with a compressive plate set on a Lloyds Instruments LR 50K. The wrench's head was locked inside a vice and leant on a steel plate to be locked vertically (Figure 9).

Figure 10 shows the force-displacement curves of the six tested parts. There is a low dispersion in the results from one part to another of the same batch, which makes the results relevant. It appears that the optimized parts are stiffer than the non-optimized ones. In fact, the optimization of the layers' fiber angles has increased the stiffness of the printed parts by a significant improvement of 18%. This proves the usefulness of the optimization process compared to an intuitive reinforcement (0°/−30°).

3.3. Comparison with an optimization model

To check whether our quick method gives a result close to the optimal solution, we compared it to a solution obtained with an optimization model.

A direct optimization model with a Non-linear Programming Quadratic Line Search (NLPQL) algorithm was used with the Ansys Workbench software. The objective is to minimize the maximal displacement. Each layer's angle was set as a parameter initialized to 0° with a range of variation between −90° and 90°. The main issue, which led us to develop the quick method presented before in the first place, is that it is difficult to implement this model with many parameters. In our case, the wrench was built

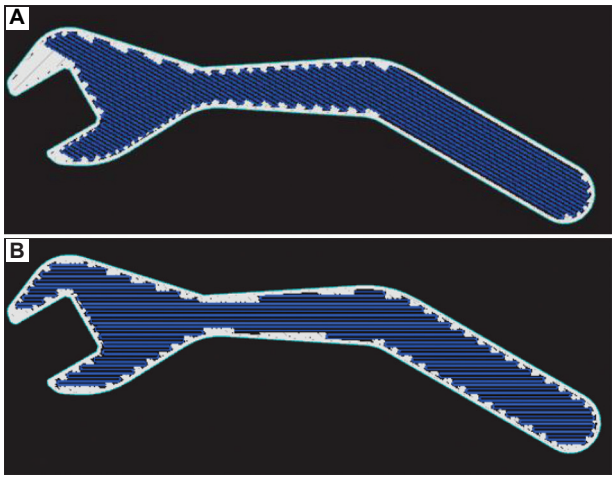

Figure 8. Printing routes with −30° oriented fibers (A) and 0° oriented fibers (B).

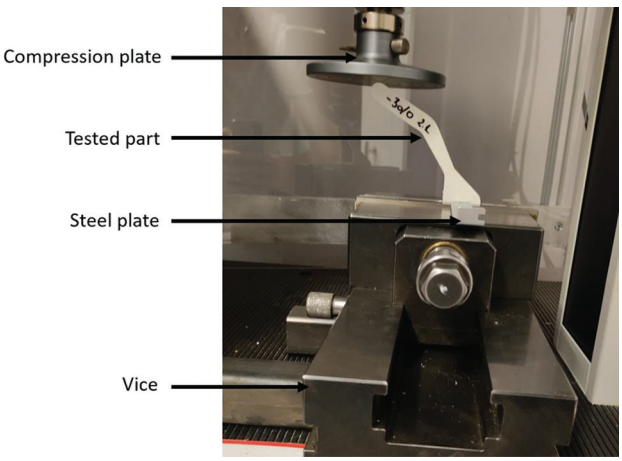

Figure 9. Testing setup.

with 60 layers, which would require 60 parameters as well. However, the mechanical case was close to a 2D problem, as the load was set in the XY-plane. This was confirmed by the fact that our code gave the same angle sequence for each stack. Thus, the direct optimization method was applied on only ten layers of the wrench. Figure 11 shows the convergence of the model, which required 11 iterations to obtain the optimal (i.e., the lowest) maximal displacement within the part. Hence, a sequence of 10° was

Table 1. Comparison of the two optimization methods

Comparison criteria	Direct optimization (NLPQL)	Fast layering optimization
Computation time	> 5 h	16 s
Resulting layering	−30°/6°/0°/−9°/20°/ −2°/−3°/14°/−4°/−33°	−2°/−28°/−20°/−15°/−11°/ −6°/6°/12°/−2°/−2°
Resulting maximal displacement	4.9554×10^{-5} m	5.4166×10^{-5} m (+9%)

NLPQL: Non-linear Programming Quadratic Line Search

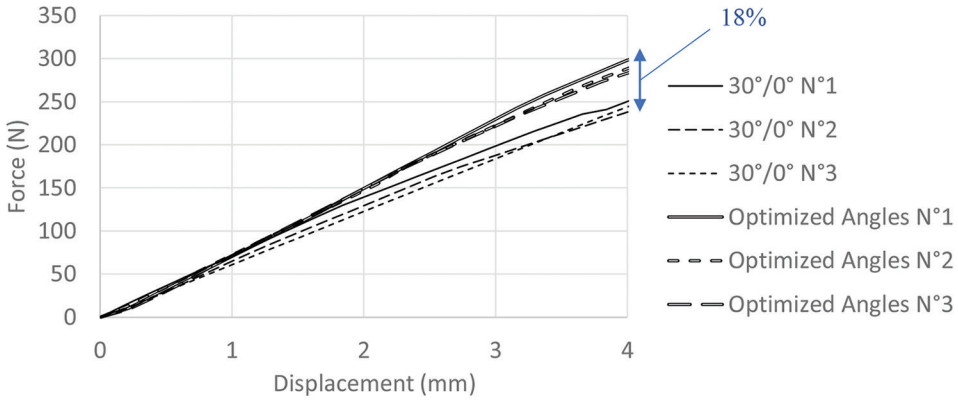

Figure 10. Force-displacement curves of the six tested parts.

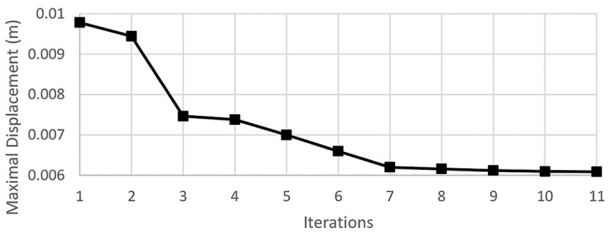

Figure 11. Convergence of the direct optimization model.

found. Then, this sequence was repeated 6 times to fill the geometry of the wrench.

A simulation on a part with the directly optimized angle sequence showed that the stiffness of the wrench is only 9% higher than the wrench obtained with our quick method, with a much higher computation time (Figure 12 and Table 1). If finding the best solution is requested, the NLPQL method is suitable but, if the goal is to quickly find an improved solution, the approach proposed in this paper is a good compromise between computation time and the search for the best solution. It is also important to note that this comparison was possible because the case was close to a 2D case. A more complex case would be harder to optimize with a gradient method due to the number of design parameters it would require. Ansys Workbench software, which was used for this study, limits, for example, the number of parameters to 20 for automatically computed Design of Experiments.

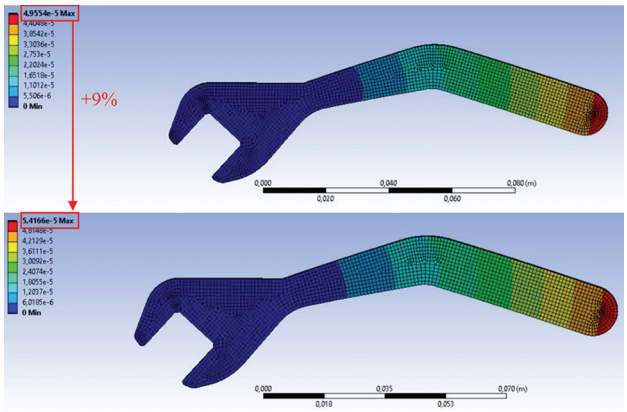

Figure 12. Displacement fields of the two compared wrenches: direct optimized (top) and quick optimized (bottom).

Hence, our quick method is a good compromise between performance and design time, as it led to a part that is only 9% less stiff than the optimal part within a minimal computation time.

4. Conclusions

A method to quickly optimize the fiber's orientations of a MEX-manufactured continuous fiber-reinforced composite was implemented with the finite element method in the Ansys Mechanical environment of programming. The use of stack-based model helped to reduce the numerical simulation time, which made the

application of a 2D method inside a 3D part possible. Moreover, the proposed model is useful to consider not only one but several reinforcement directions.

The method relies on the fact that a continuous fiber is optimally used when oriented parallel to the stress flow. This is due to the high anisotropy of fibers and their exceptional tensile properties compared to polymers. Yet, continuous fiber-reinforced filaments are expensive, so this work also proposes a method to optimize the number of reinforced layers and therefore optimize the cost of the manufactured parts. The application of the stack-based layering optimization on printed parts gave satisfying results, with the stiffness of the parts being only 9% lower than the one found with a time-costly direct optimization method.

The next step would be to consider a more flexible approach based on curved fiber routes rather than unidirectional ones. The development of slicer software to customize the fiber routes is warranted since this flexibility has yet to be incorporated into the commercial printers.

Acknowledgments

None.

Funding

This research did not receive any specific grant from funding agencies in the public, commercial, or not-for-profit sectors.

Conflict of interest

The authors declare that they have no known competing financial interests or personal relationships that could have appeared to influence the work reported in this paper.

Author contributions

Conceptualization: Valentin Marchal, Yicha Zhang, Nadia Labed, and François Peyraut
Data curation: Valentin Marchal
Formal analysis: Valentin Marchal, Nadia Labed, and François Peyraut
Funding acquisition: Yicha Zhang
Investigation: Valentin Marchal and Rémy Lachat
Methodology: All authors
Software: Valentin Marchal
Supervision: Yicha Zhang, Nadia Labed, and François Peyraut
Validation: Rémy Lachat
Visualization: Valentin Marchal
Writing – original draft: Valentin Marchal, Yicha Zhang, and François Peyraut
Writing – review and editing: All authors

Ethics approval and consent to participate

Not applicable.

Consent for publication

Not applicable.

Availability of data

The data are not publicly available because the research work was carried out in a laboratory whose scientific developments are protected and cannot be transferred. However, the experimental data proving the relevance of the proposed numerical method are available from the corresponding author on reasonable request.

References

1. Zheng H, Zhang W, Li B, *et al.*, 2022, Recent advances of interphases in carbon fiber-reinforced polymer composites: A review. *Compos B Eng*, 233: 109639.

   https://doi.org/10.1016/j.compositesb.2022.109639

2. Li J, Durandet Y, Huang X, *et al.*, 2022, Additively manufactured fiber-reinforced composites: A review of mechanical behavior and opportunities. *J Mater Sci Technol*, 119: 219–244.

   https://doi.org/10.1016/j.jmst.2021.11.063

3. Liao G, Li Z, Cheng Y, *et al.*, 2018, Properties of oriented carbon fiber/polyamide 12 composite parts fabricated by fused deposition modeling. *Mater Des*, 139: 283–292.

   https://doi.org/10.1016/j.matdes.2017.11.027

4. Yan C, Hao L, Xu L, *et al.*, 2011, Preparation, characterisation and processing of carbon fibre/polyamide-12 composites for selective laser sintering. *Compos Sci Technol*, 71: 1834–1841.

   http://dx.doi.org/10.1016/j.compscitech.2011.08.013

5. Goodridge RD, Shofner ML, Hague RJM, *et al.*, 2011, Processing of a polyamide-12/carbon nanofiber composite by laser sintering. *Poly Test*, 30: 94–100.

   http://dx.doi.org/10.1016/j.polymertesting.2010.10.011

6. Jansson A, Pejryd L, 2016, Characterisation of carbon fibre-reinforced polyamide manufactured by selective laser sintering. *Addit Manuf*, 9: 7–13. http://dx.doi.org/10.1016/j.addma.2015.12.003

7. Hofstätter T, Pedersen DB, Tosello G, *et al.*, 2017, Applications of fiber-reinforced polymers in additive manufacturing. *Procedia CIRP*, 66: 312–316.

   https://doi-org.ezproxy.utbm.fr/10.1016/j.procir.2017.03.171

8. Tekinalp HL, Kunc V, Velez-Garcia GM, *et al.*, 2014, Highly oriented carbon fiber-polymer composites via additive manufacturing. *Compos Sci Technol*, 105: 144–150.

   http://dx.doi.org/10.1016/j.compscitech.2014.10.009

9. van de Werken N, Tekinalp H, Khanbolouki P, *et al.*, 2020, Additively manufactured carbon fiber-reinforced composites: State of the art and perspective. *Addit Manuf*, 31: 100962.

   https://doi.org/10.1016/j.addma.2019.100962

10. Tian X, Liu T, Yang C, *et al.*, 2016, Interface and performance of 3D printed continuous carbon fiber reinforced PLA composites. *Composites Part A*, 88: 198–205.

    http://dx.doi.org/10.1016/j.compositesa.2016.05.032

11. Aravind AU, Bhagat AR, Radhakrishnan R, *et al.*, 2020, A novel use of twisted continuous carbon fibers in additive manufacturing of composites. *Materials Today: Proceedings*.

    https://doi.org/10.1016/j.matpr.2020.07.665

12. Material Datasheet: Composites, Markforged. Available from: https://www-objects.markforged.com/craft/materials/compositesv5.2.pdf [Last accessed on 2022 Dec 13].

13. Mahajan C, Cormier D, 2015, 3D Printing of Carbon Fiber Composites with Preferentially Aligned Fibers. Proceedings of the 2015 Industrial and Systems Engineering Research Conference.

14. Goh GD, Toh W, Yap YL, *et al.*, 2021, Additively manufactured continuous carbon fiber-reinforced thermoplastic for topology optimized unmanned aerial vehicle structures. *Composites Part B*, 216: 108840.

    https://doi.org/10.1016/j.compositesb.2021.108840

15. Lewicki JP, Rodriguez JN, Zhu C, *et al.*, 2017, 3D-Printing of meso-structurally ordered carbon fiber/polymer composites with unprecedented orthotropic physical properties. *Sci Rep*, 7: 43401.

    https://doi.org/10.1038/srep43401

16. Zhou Y, Nomura T, Saitou K, 2018, Multi-component topology and material orientation design of composite structures (MTO-C). *Comput Methods Appl Mech Eng*, 342: 438–457.

    https://doi.org/10.1016/j.cma.2018.07.039

17. Ding H, Xu B, 2021, A novel discrete-continuous material orientation optimization model for stiffness-based concurrent design of fiber composite. *Compos Struct*, 273: 114288.

    https://doi.org/10.1016/j.compstruct.2021.114288

18. Li Y, Xu K, Liu X, *et al.*, 2021, Stress-oriented 3D printing path optimization based on image processing algorithms for reinforced load-bearing parts. *CIRP Ann Manuf Technol*, 70: 195–198.

    https://doi.org/10.1016/j.cirp.2021.04.037

19. Safonov AA, 2019, 3D topology optimization of continuous fiber-reinforced structures via natural evolution method. *Compos Struct*, 215: 289–297.

    https://doi.org/10.1016/j.compstruct.2019.02.063

20. Nomura T, Kawamoto A, Kondoh T, *et al.*, 2019, Inverse design of structure and fiber orientation by means of topology optimization with tensor field variables. *Composites Part B*, 176: 107187.

    https://doi.org/10.1016/j.compositesb.2019.107187

21. Jung T, Lee J, Nomura T, *et al.*, 2022, Inverse design of three-dimensional fiber-reinforced composites with spatially-varying fiber size and orientation usign multiscale topology optimization. *Compos Struct*, 279: 114768.

    https://doi.org/10.1016/j.compstruct.2021.114768